An Electrochemical Biosensor for Sensitive Detection of MicroRNA-155: Combining Target Recycling with Cascade Catalysis for Signal Amplification

Xiaoyan Wu, Yaqin Chai,* Pu Zhang, and Ruo Yuan*

Key Laboratory of Luminescent and Real-Time Analytical Chemistry (Southwest University), Ministry of Education, College of Chemistry and Chemical Engineering, Southwest University, Chongqing 400715, P. R. China

Ⓢ Supporting Information

ABSTRACT: In this work, a new electrochemical biosensor based on catalyzed hairpin assembly target recycling and cascade electrocatalysis (cytochrome c (Cyt c) and alcohol oxidase (AOx)) for signal amplification was constructed for highly sensitive detection of microRNA (miRNA). It is worth pointing out that target recycling was achieved only based on strand displacement process without the help of nuclease. Moreover, porous TiO_2 nanosphere was synthesized, which could offer more surface area for Pt nanoparticles (PtNPs) enwrapping and enhance the amount of immobilized DNA strand 1 (S1) and Cyt c accordingly. With the mimicking sandwich-type reaction, the cascade catalysis amplification strategy was carried out by AOx catalyzing ethanol to acetaldehyde with the concomitant formation of high concentration of H_2O_2, which was further electrocatalyzed by PtNPs and Cyt c. This newly designed biosensor provided a sensitive detection of miRNA-155 from 0.8 fM to 1 nM with a relatively low detection limit of 0.35 fM.

KEYWORDS: microRNA, dual signal amplification, target catalyzed hairpin assembly, cascade catalysis
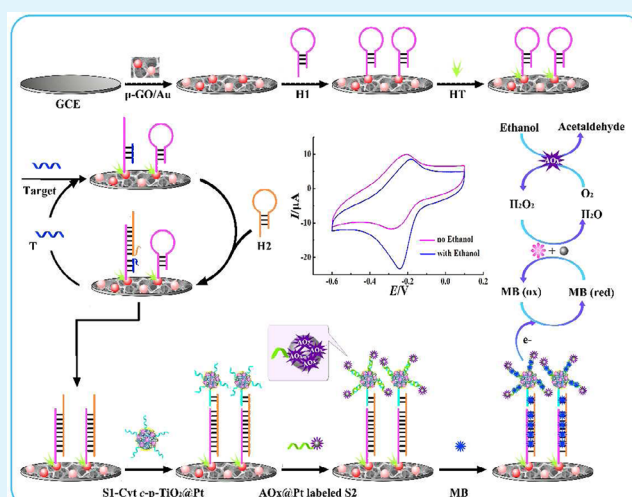
1. INTRODUCTION

MicroRNAs (miRNAs), a large family of endogenous and small (∼18−25 nucleotides) noncoding RNAs, have attracted tremendous interest as clinically important biomarkers or drug discovery targets for cancers (stomach, prostate, lung, breast, pancrea, colon, etc.) and other diseases (chronic lymphocytic leukemia, diabetes, heart diseases, etc.).[1,2] Sensitive and accurate detection of miRNA is a prospective requirement, which is helpful to understand the disease-related biological processes.[3] However, methods for miRNAs detection are predominantly cloning, northern blotting, and microassay analysis, which usually have some limitations, such as poor sensitivity, time-consuming, expensive, and complicated instruments.[4,5] In recent years, electrochemical biosensors have held great promise due to the inherent advantages of facility, low-cost, fast response time, and high sensitivity.[6] So far, various electrochemical miRNA biosensors have been fabricated.[7−9] Because of the low abundance of miRNAs, which are at the attomolar to femtomolar level in biological samples,[10] the desire to enhance the detection sensitivity by coupling various amplification strategies is rather intense.

On the one hand, numerous electrochemical nucleic acid methods of detection have focused on using nanostructured conducting material as support matrix to improve the sensitivity of the sensors.[11−13] On the other hand, a variety of DNA signal amplification strategies have been reported to enhance the detection signal.[14,15] In general, signal amplification can be achieved by nanomaterials, enzyme catalytic reaction, and target recycling reaction. Recently, owing to their large surface area and versatile porous structure, nanoporous materials have been applied in biosensing.[16,17] Their superior properties are beneficial for loading massive molecules and accelerating diffusion rate. Inspired by this perspective, novel porous graphene oxide/Au (GO/Au) composites were synthesized in this work, which possessed considerably improved specific surface area, excellent electrical conductivity, and unique biocompatibility. Besides, nanoporous TiO_2 with good biocompatibility and chemical/thermal stability can offer more surface area for the loading of Pt nanoparticles (PtNPs). Thus, PtNP-functionalized nanoporous TiO_2 material (p-TiO_2@PtNPs) was employed as signal amplification enhancer. It is worth pointing out that this hybrid material

Table 1. All DNA and miRNA Sequences Used in the Experiment

name	sequence (5′ to 3′)
MiRNA-155 (T)	UUAAUGCUAAUCGUGAUAGGGGU
hairpin probe H1	TAATCGTGATAGGGGTATGGACATGGAACCCCTATCACGATTAGCATTAAAGA-SH
hairpin probe H2	ATGGACATGGATAATCGTGATAGGGGTTCCATGTCCATACCCCTATGAAGGAGCGACT
DNA strand S1	SH-TTAGTCGCTCCT
DNA strand S2	SH-GGAGCGACT
thrombin aptamer (nDNA)	GGTTGGTGTGGTTGG
microRNA-101 (nRNA)	UACAGUACUGUGAUAACUGAA
single-base difference miRNA (sRNA)	UUAAGGCUAAUCGUGAUAGGGGU

not only retains the electrocatalytic activity of PtNPs but also possesses enhanced electrochemical sensing ability toward H_2O_2.[18] Moreover, this material can also immobilize large amount of DNA strand S1 and cytochrome c (Cyt c), which is a typical metalloprotein possessing pseudoperoxidase activity that can catalytically reduce H_2O_2.[19,20] In addition, enzyme-signal amplification, especially cascade catalysis amplification using (pseudo) bienzyme labeled probe, is expected to improve detection sensitivity.[21,22] Herein, the combination of alcohol oxidase (AOx) and Cyt c for cascade catalysis amplification catches our eager attention. AOx, an oligomeric enzyme with eight identical subunits, is responsible for the oxidation of low molecular weight alcohol (such as ethanol) to the corresponding aldehyde, using molecular oxygen (O_2) as electron acceptor and producing H_2O_2. Because of the property of AOx, it is mainly used as a biorecognition element in ethanol biosensors, but it is rarely applied in electrochemical miRNA biosensor.[23] In addition, AOx catalyzing ethanol to generate H_2O_2 is a relatively "slow" process, so that it is likely to slow the equilibration process and prevent large amounts of H_2O_2 from leaving the sensing membranes.[24] That is to say, the slow process will be useful to the next cycle (the reduction of H_2O_2), improving the catalysis efficiency. Thus, it is promising to use AOx catalyzing ethanol to generate H_2O_2 in this system.

Taking into account the above advantages and catalyzed hairpin assembly (CHA) target recycling,[25,26] we designed a novel cascade catalysis amplified electrochemical biosensor for miRNA-155 detection. Herein, porous GO/Au composites were employed for the immobilization of capture hairpin probe H1. With the help of target, the capture probe H1 hybridized with target to open its hairpin structure. The target that had been hybridized with H1 could be displaced from the structure in the presence of another stable hairpin DNA H2. The released target was available for initiating next cycle, which was promising for signal amplification. Then a large number of H1−H2 duplex was produced after the cyclic process. The newly emerging DNA part (residual simple stranded fragment of H2) could bind with DNA S1-conjugated biobarcode NPs (S1-Cyt c-p-TiO$_2$@PtNPs). Finally, AOx@Pt labeled DNA S2 hybridized with S1 to modify the electrode surface. To achieve detection of miRNA, a mass of methylene blue (MB) as electron mediator was intercalated into DNA duplex.[27,28] Therefore, a cascade catalysis amplified miRNA biosensor was successfully designed based on AOx, Cyt c, and PtNPs. In the presence of ethanol, AOx effectively catalyzed the oxidation of ethanol to acetaldehyde, accompanied with the generation of H_2O_2 by using dissolved O_2. Then, Cyt c and PtNPs cooperatively catalyzed the reduction of H_2O_2, resulting in an extremely high sensitivity with detection limit of 0.35 fM for miRNA-155. This strategy provided a general and promising way for sensitive detection of miRNAs in clinical applications.

2. EXPERIMENTAL SECTION

2.1. Materials and Reagents. Graphene oxide (GO) was obtained from Nanjing Xianfeng Nano Co. (Nanjing, China). Alcohol oxidase (AOx, EC 1.1.3.13, from pichiapastoris), bovine heart cytochrome c (Cyt c), tetrabutoxytitanium, (3-aminopropyl)tri-methoxy silane (APTMS), hexanethiol (96%, HT), gold chloride (HAuCl$_4$), chloroplatinic acid (H$_2$PtCl$_6$), and MB were purchased from Sigma-Aldrich Chem. Co. (St. Louis, MO, U.S.A.). Trishydroxy-methylaminomethane hydrochloride (Tris-HCl) was supplied by Roche (Switzerland). All other chemicals were of reagent grade and used as received. DNA and miRNA sequences were synthesized and purified by Sangon (Shanghai, China) and TaKaRa (Dalian, China), respectively. The sequences are shown in Table 1.

Buffers involved in this work were as follows: 1 × TE buffer (10 mM Tris-HCl, 1.0 mM ethylenediaminetetraacetic acid (EDTA), pH 8.0) was used for dissolving all oligonucleotides. Probe immobilization buffer (IB): 10 mM Tris-HCl, 1.0 mM EDTA, 10 mM TCEP, 0.1 M NaCl (pH 7.4), DNA hybridization buffer (HB1): 10 mM Tris-HCl, 1.0 mM EDTA, 1.0 M NaCl (pH 7.0), miRNA hybridization buffer (HB2): 10 mM Tris-HCl, 1.0 mM EDTA, 0.2 M NaCl, 10 mM MgCl$_2$ (pH 8.0), working buffer: 0.1 M phosphate buffered solutions (PBS, pH 7.0) containing 10 mM Na$_2$HPO$_4$, 10 mM NaH$_2$PO$_4$, and 2.0 mM MgCl$_2$. Ultrapure water (specific resistance of 18 MΩ·cm) was employed throughout the study.

2.2. Apparatus and Measurements. All electrochemical measurements, including cyclic voltammetry (CV) and differential pulse voltammetry (DPV), were performed with a CHI 660D electrochemical workstation (Shanghai Chenhua Instrument, China). All experiments were conducted on a conventional three-electrode system comprised of a platinum wire as auxiliary electrode, a saturated calomel electrode (SCE) as reference electrode, and a modified glassy carbon electrode (GCE,Φ = 4 mm) as working electrode. The scanning electron micrographs were taken with scanning electron microscope (SEM, S-4800, Hitachi, Japan). CV measurements were taken in 2 mL of PBS (0.1 M) containing 5.0 mM $[Fe(CN)_6]^{3-/4-}$ with potential range from −0.2 to 0.6 V at a scan rate of 50 mV s^{-1}. DPV measurements were carried out in 2 mL of PBS (0.1 M, pH 7.0) containing 120 μL of absolute ethanol. The parameters applied were: potential range from −0.6 to 0.1 V, 50 mV modulation amplitude, 50 ms pulse width, and 0.2 s pulse period.

2.3. Preparation of Porous GO/Au Composites. The porous GO/Au composites were prepared according to previously reported procedure by hydrothermal method with slight modifications.[29] GO was dissolved in water with the concentration of 0.5 mg mL^{-1} to form homogeneous GO solution by sonication for 1 h. Subsequently, 10 mL of GO, 200 μL of HAuCl$_4$ (1%), and 20 μL of polyethylene glycol (PEG, 1%) were mixed uniformly in ultrasonic bath for 1 h. After it reacted at 180 °C for 12 h and cooled to room temperature, the mixture was washed several times with water. Through freeze-drying process, the porous GO/Au composites were obtained. Finally, the products were redispersed in PBS.

2.4. Preparation of Citrate-Stabilized PtNPs. Citrate-stabilized PtNPs were prepared according to the reported procedure with slight modification.[30] Briefly, 1 mL of 1% H$_2$PtCl$_6$ aqueous solution was added into 100 mL of water and then heated to boiling. Sequentially, 3 mL of 1% sodium citrate aqueous solution was immediately added into
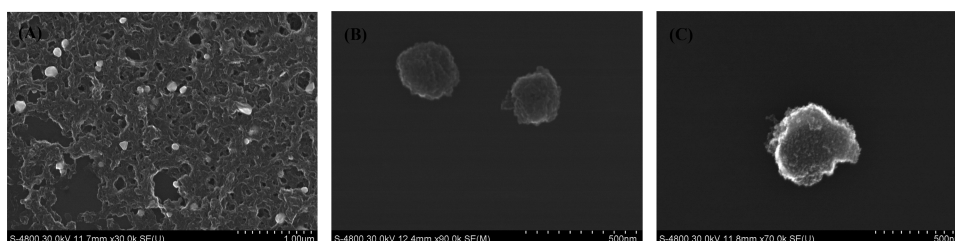
Scheme 1[a]

[a](A) The preparation process of the biobarcode conjugate labels. S1 and Cyt c are attached to the p-TiO₂@PtNPs. (B) Schematic representation of the proposed strategy for miRNA-155 detection. (C) Structures of H1, target, and H2.

the mixture, keeping it at boiling temperature for approximately 30 min. After the solution cooled to room temperature slowly, dark brown colloidal PtNPs were obtained.

2.5. Preparation of Nanoporous TiO₂@Pt Materials (p-TiO₂@PtNPs). The preparation of p-TiO₂@PtNPs was accomplished by following the procedure reported in previous literature, with minor modifications.[31] First, 1 mL of tetrabutoxytitanium was added to 25 mL of ethylene glycol and was magnetically stirred for 8 h at room temperature. Then, the mixture was rapidly poured into 90 mL of acetone bath containing a small amount of water under vigorous stirring for 1 h. By centrifuging and washing with distilled water and ethanol several times, the white precipitate was obtained. Second, the as-synthesized particles were redispersed in water to form stable suspensions and were heated to reflux under stirring. After refluxing for 1 h, the white precipitate was harvested by centrifugation, followed by washing with water several times and drying at 50 °C. Thus, nanoporous TiO₂ (p-TiO₂) was synthesized successfully.

Subsequently, approximately 100 mg of as-synthesized p-TiO₂ was dispersed into 40 mL of ethanol. Then, 400 μL of APTMS, 2 mL of water, and 2 mL of ammonia were added to the above stable suspension gradually. After the suspension was continuously stirred for 10 h, the functionalized p-TiO₂ was collected by centrifuging and washing extensively and dispersed in 10 mL of water finally. Following that, excess as-prepared PtNPs colloid was added in 0.5 mL of surface-functionalized p-TiO₂. The mixture was sonicated for 30 min and then left for 12 h at room temperature. By centrifuging the mixture, product of p-TiO₂@PtNPs was obtained and dissolved in 5 mL of water to form gray and stable suspension.

2.6. Preparation of S1-Conjugated Biobarcode NPs (S1-Cyt c-p-TiO₂@PtNPs). In brief, 200 μL of thiol-modified S1 (2 μM) was mixed with 1 mL of as-prepared p-TiO₂@PtNPs and stirred gently overnight at 4 °C. Afterward, 1 mg of Cyt c that was suspended in 1 mL of Tris-HCl buffer was added for blocking, and the mixture was allowed to further react for another 4 h at 4 °C. The product was

Figure 1. SEM images of (A) porous GO/Au composites, (B) p-TiO$_2$, and (C) p-TiO$_2$@Pt.

obtained by centrifuging, washing, and recentrifuging, followed by dispersal in 1 mL of Tris-HCl buffer.

2.7. Preparation of AOx@Pt Labeled S2. Briefly, 200 μL of thiol-modified S2 (2 μM) was added into 2 mL of as-prepared PtNPs and kept overnight under slow stirring at 4 °C. Following that, superfluous AOx was mixed with the above-obtained solution. After the solution stirred for 5 h, the resulting AOx@Pt-labeled S2 solution was centrifuged and washed three times with water. The obtained composite was resuspended in Tris-HCl buffer and stored at 4 °C before use.

2.8. Fabrication of the miRNA Biosensor. Prior to use, all the hairpin oligonucleotides were annealed by warming the solution to 95 °C for 2 min and then slowly cooling to room temperature. First of all, a GCE was carefully polished with 0.3 and 0.05 μm alumina slurries to obtain a mirrorlike surface, then sonicated in water, ethanol, and water for 2 min each, and then dried in air at room temperature. Then, 6 μL of porous GO/Au composites were cast onto the electrode surface to form a uniform film by drying in air at room temperature. Next, 10 μL of thiol-modified H1 (2 μM) was attached onto the porous GO/Au layer surface for 16 h at room temperature, resulting in assembling H1 on the modified electrode via Au−S affinity. After that, the modified electrode was rinsed with ultrapure water and blocked with 10 μL of HT (1.0 mM) for 40 min to prevent nonspecific adsorption. Subsequently, 10 μL of mixture containing different concentrations of target miRNA and H2 (2 μM) was dripped onto the modified electrode and incubated for 2 h at 37 °C. After rinsing with ultrapure water, the modified electrode was incubated with 10 μL of S1-Cyt c-p-TiO$_2$@PtNPs for 2 h at 4 °C. This was followed by washing, drying, and further incubating with AOx@Pt labeled S2 at 4 °C. Ultimately, 10 μL of MB (1.0 mM) was intercalated into the double-stranded DNA (dsDNA) polymers through electrostatic interaction and then served as an electron mediator, which gave the electrochemical signal and accordingly quantitative criteria for miRNA detection.

3. RESULTS AND DISCUSSION

3.1. Mechanism of the Proposed Biosensor. Scheme 1 illustrated the general principle of cascade catalysis amplification-based electrochemical biosensor for the detection of miRNA. Two hairpin DNA segments (H1 and H2) were employed in CHA process.[32] They could not automatically hybridize with each other in absence of target, only maintaining the sufficiently stable stem-loop structure (see Supporting Information S1). First, the 3′-thiol-modified hairpin DNA H1 was assembled on porous GO/Au composite-modified GCE surface through Au−S bond. Then, the introduction of target miRNA could hybridize with H1 and open its stem-loop structure to form dsDNA, as well as made the complementary sequence of H1 to another hairpin DNA H2 exposed. In the presence of H2, the binding of H1 with H2 emerged through a branch migration process.[33−35] Because the H1−H2 duplex was longer and more stable than the H1−T hybrids, the H2 would replace and liberate the target when it hybridized with H1. The released target became available for the next hybridization cycle with H2 (the specific mechanism of CHA; see Supporting Information S2). Afterward, each target miRNA could undergo

many cycles, resulting in many newly emerging DNA fragment (the sticky end of H2). The residual simple-stranded fragment of H2 could further hybridize with DNA S1 on biobarcode, which was functionalized by Cyt c-p-TiO$_2$@PtNPs, and then led to the successful immobilization of AOx@Pt labeled S2. Eventually, a large amount of MB molecules was intercalated into the dsDNA polymers through electrostatic interaction to achieve an electrochemical signal.[36] Herein, a cascade catalysis amplified miRNA biosensor was successfully designed based on the AOx, Cyt c, and PtNPs. In the presence of ethanol, AOx catalyzed the oxidation of ethanol to acetaldehyde, accompanied with the generation of H$_2$O$_2$. Subsequently, Cyt c and PtNPs further catalyzed the reduction of H$_2$O$_2$ effectively, which led to an enormous amplified electrochemical signal. Therefore, the sensitivity of the proposed miRNA biosensor could be dramatically enhanced by simultaneously using target recycling and cascade catalysis as signal amplification protocol.

3.2. Characterization of the Different Nanomaterials. The morphology of the as-prepared different nanomaterials was presented in Figure 1. It was clearly found that a porous structure of GO and good dispersity of Au nanoparticles (AuNPs) were obtained from the SEM image (Figure 1A). AuNPs were uniformly distributed not only on the surface but also inside the GO, which was beneficial for capturing probe attachment and electronic transmission rate. Seen from Figure 1B, the as-prepared p-TiO$_2$ possessed uniform size with an average diameter of 250 nm. The rough surface of p-TiO$_2$ nanospheres provided a large surface area to load more PtNPs. Compared with the p-TiO$_2$ nanospheres, many bright dots spread along the nanoporous spheres could be observed in Figure 1C, which were PtNPs. This reveals that p-TiO$_2$@PtNPs were prepared successfully.

3.3. Electrochemical Characterization of the Proposed Biosensor. The assembly process of the modified electrode was investigated by CV in Figure 2. Clearly, the bare GCE exhibited a well-defined redox peak of [Fe(CN)$_6$]$^{3-/4-}$ (curve a). When the porous GO/Au composites were modified on the GCE surface, the peak current apparently increased (curve b), because the conductive AuNPs could accelerate the electron transfer. After capture probe H1 was assembled onto the electrode surface, a dramatic decrease in peak current was noted (curve c), accounting for the fact that H1 can hinder the diffusion of ferricyanide toward the electrode surface. Non-conductive HT as blocking agent made the peak current decrease again (curve d). Additionally, the peak current further decreased after incubating the mixture of target (10 pM) and H2 (curve e), which was attributed to the successful CHA process and the fact that more negatively charged DNA strands were loaded on the electrode surface, inhibiting the diffusion of redox probe. Afterward, the peak current decreased successively after immobilizing DNA S1 on biobarcode (curve f) and
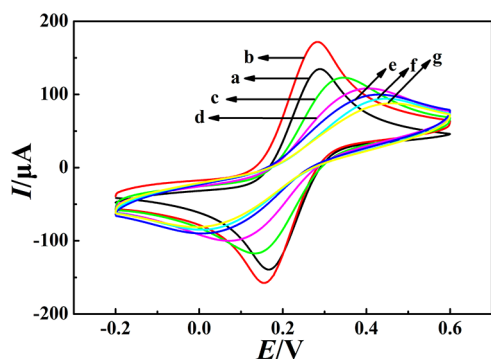
Figure 2. CVs for each immobilized step in 5 mM $K_3Fe(CN)_6$ solution containing 0.1 M KCl: (a) bare GCE, (b) p-GO/Au modified GCE, (c) step b assembled H1, (d) step c blocked with HT, (e) step d incubated with the mixture of T and H2, (f) step e hybridized with S1-conjugated biobarcode NPs, and (g) step f hybridized with AOx@Pt labeled S2.

hybridizing with AOx@Pt labeled S2 (curve g), attributed to the increase of steric hindrance.

3.4. Comparison of Different Signal-Amplification Strategies. To test the signal amplification of the proposed protocol, the miRNA biosensor was utilized with different signal amplification strategies (Figure 3). The change of current responses ($\Delta I = I - I_0$, where I_0 and I are current responses before and after bioelectrocatalysis, respectively) was employed to evaluate the effect of different strategies. Herein, all the assay procedures were performed with the same concentration of target miRNA (10 pM). As shown in Figure 3A, it was clear to obverse a ΔI of 3.69 μA when the biosensor was incubated with S1/PtNPs only, because PtNPs could catalyze H_2O_2. Besides,

when the biosensor was incubated with S1-Cyt c-p-TiO$_2$@PtNPs (Figure 3B), the ΔI was enhanced to 5.86 μA, owing to the cooperatively catalytic ability of Cyt c and PtNPs. This phenomenon also indicated the fact that p-TiO$_2$@PtNPs hybrid nanomaterial possessed enhanced catalytic ability toward H_2O_2, because the p-TiO$_2$ nanomaterials with good biocompatibility and large surface area could significantly increase the amount of PtNPs assembly for signal amplification. More inspiringly, the ΔI was remarkably increased to 9.86 μA when the biosensor was successively incubated with S1-Cyt c-p-TiO$_2$@PtNPs and AOx@Pt-labeled S2 (Figure 3C). The reason for this was that cascade catalysis of AOx, Cyt c, and PtNPs could enormously enhance the current response. The comparison results displayed that excellent nanomaterial (p-TiO$_2$@PtNPs) and cascade catalysis of AOx and Cyt c were crucial for final enhancement of detection sensitivity.

3.5. Performance of the miRNA Biosensor. Under the optimized experimental conditions (see Supporting Information S3), the analytical performance of the proposed biosensor in detecting miRNA-155 with different concentrations is shown in Figure 4. The electrochemical signal gradually increased with increasing concentrations of miRNA-155 in 1 mL of PBS (0.1 M, pH 7.0) containing 120 μL of absolute ethanol (Figure 4A). The resulting calibration plots for quantitative determination of miRNA-155 were illustrated in Figure 4B. The peak current was proportional to the logarithm concentration of miRNA-155 over a 7 orders of magnitude range from 0.8 fM to 1 nM with a linear correlation coefficient of 0.9964 and a detection limit of 0.35 fM (defined as signal-to-noise ratio of three times). It revealed that the proposed biosensor was efficient for sensitive detection of miRNA-155, which was attributed to the employment of CHA target recycling, huge loading of PtNPs
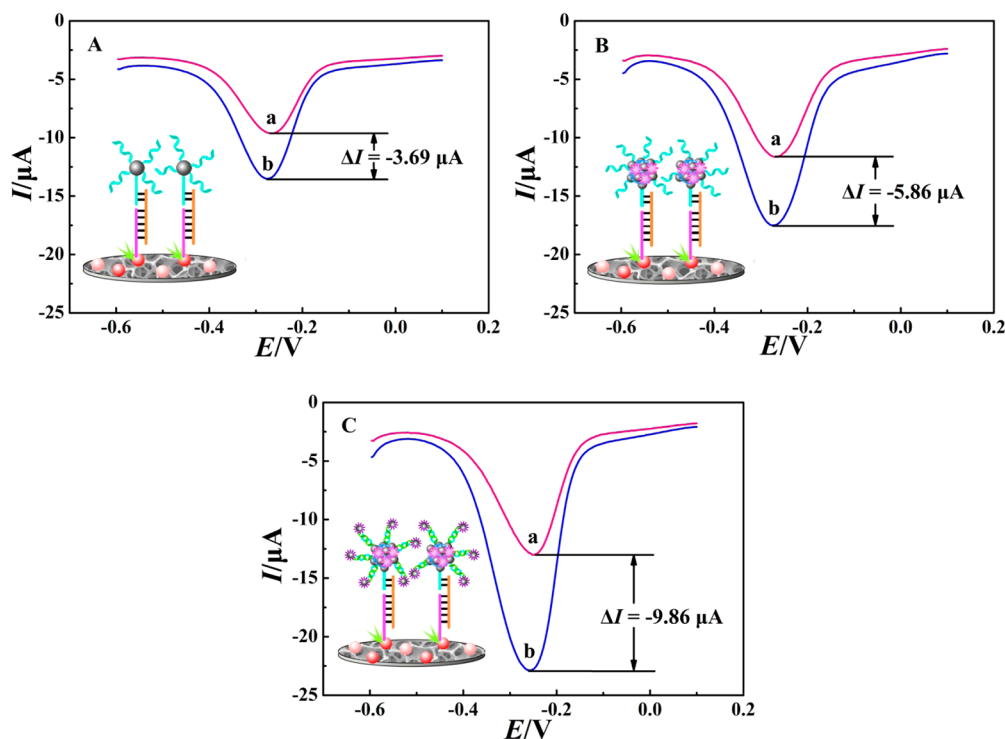

Figure 3. DPV responses of the as-prepared miRNA biosensor before (a) and after (b) bioelectrocatalysis, according to different signal-amplification strategies: (A) catalysis of PtNPs; (B) cooperative catalysis of Cyt c and p-TiO$_2$@PtNPs; (C) cascade catalysis of Cyt c, p-TiO$_2$@PtNPs and AOx. (A) and (B) were detected in 1 mL of PBS containing 1.8 mM H_2O_2, while (C) was detected in 1 mL of PBS (pH 7.0) containing 120 μL of absolute ethanol.

717

dx.doi.org/10.1021/am507059n | ACS Appl. Mater. Interfaces 2015, 7, 713–720
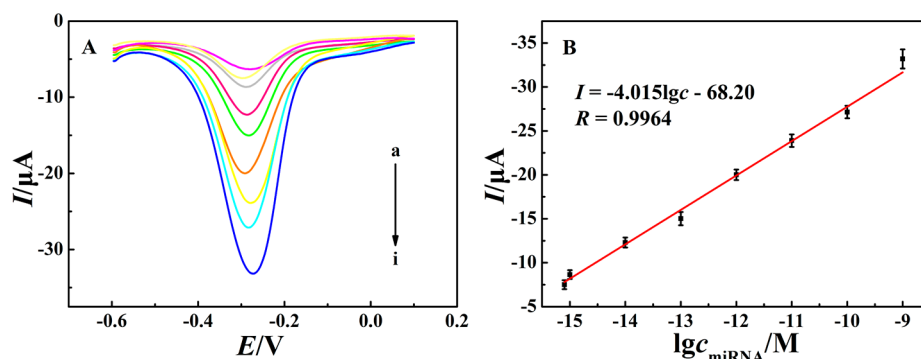
Figure 4. (A) DPV responses of the proposed biosensor with different miRNA-155 concentrations in 1 mL of PBS (pH 7.0) containing 120 μL of absolute ethanol: (a) 0 fM, (b) 0.8 fM (c) 1 fM, (d) 10 fM, (e) 100 fM, (f) 1 pM, (g) 10 pM, (h) 100 pM, (i) 1 nM. (B) The calibration plots of DPV peak current vs the logarithm of miRNA-155 concentration.

based on numerous amine groups modified p-TiO$_2$ nanomaterial, and the cascade bioelectrocatalysis of AOx, Cyt c, and PtNPs. Table 2 compared the performance of our proposed

Table 2. Analytical Performance Compared with Other Works for miRNA Detection

analytical method[a]	linear range	detection limit	ref
SPR	10 fM−1 pM	10 fM	37
ECL	100 fM−100 nM	21.7 fM	38
fluorescence	0.06 pM−12 pM	14.7 nM	39
chronoamperometry	10 fM−5 pM	3 pM	40
SWV	50 fM−30 pM	12 fM	41
DPV	100 fM−1 nM	99.2 fM	42
DPV	0.8 fM−1 nM	0.35 fM	this work

[a]SPR: surface plasmon resonance; ECL: electrochemiluminescence; SWV: square-wave voltammetry; DPV: differential pulse voltammetry.

miRNA biosensor with other works. As shown, we can see that the detection limit of the proposed miRNA biosensor was comparable and even better than those of other reported methods.

3.6. Specificity, Stability, and Reproducibility of the Proposed Biosensor. The specificity of the proposed biosensor was evaluated by incubation with the perfect complementary sequence (1 pM), noncomplementary DNA (nDNA, 10 pM), noncomplementary miRNA (nRNA, 10 pM), and single-base difference miRNA (sRNA, 10 pM), respectively. As summarized in Figure 5A, with an excess (10-fold)

amount of nontarget analytes, the proposed biosensor exhibited negligible interference to nDNA, nRNA, and sRNA. This indicated that the specificity of the proposed biosensor was acceptable.

The stability was examined by the CV signal of MB before the addition of catalytic substrate, which is aimed to demonstrate the stability of intercalated MB (Figure 5B). Through employing one proposed biosensor for 50 consecutive cyclic scans, a 3.48% decrease of initial response was found. This suggested that the intercalated MB, which served as electron mediator in this miRNA biosensor, had satisfying stability. The reproducibility of the proposed biosensor was investigated by analysis of the same concentration of miRNA-155 (1 pM) using four electrodes in the same conditions. Similar electrochemical signals and a relative standard deviation (RSD) of 5.90% were acquired. This result demonstrated the acceptable reproducibility of the proposed biosensor.

3.7. Analytical Application of the Proposed miRNA Biosensor. To monitor the reliability of the proposed biosensor, recovery experiments were performed by adding various concentrations of miRNA-155 into the 10-fold diluted healthy human serum (obtained from the Ninth People's Hospital of Chongqing, China). As anticipated from Table 3, the recovery and the RSD were ranging from 93.98% to 100.5% and from 2.13% to 6.56%, respectively, which indicated that the proposed biosensor was available for determining miRNA-155 in real biological samples.
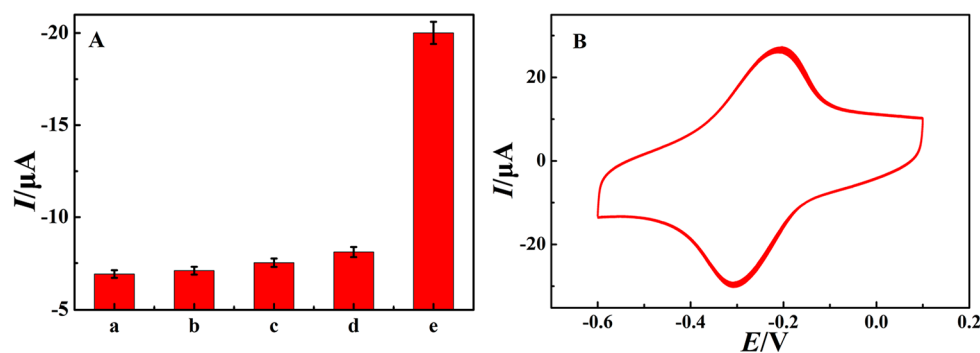

Figure 5. (A) Specificity of the proposed miRNA biosensor against different interferences: (a) blank solution (0 fM miRNA-155), (b) 10 pM nDNA, (c) 10 pM nRNA, (d) 10 pM sRNA, (e) 1 pM target miRNA-155. (B) Stability of the proposed miRNA biosensor with CV technique at a scan rate of 50 mV s^{-1}.

Table 3. Determination of miRNA-155 Added in Human Serum ($n = 3$) with the Proposed Biosensor

serum sample	added, M	found, M	recovery, %	RSD, %
1	5×10^{-15}	4.97×10^{-15}	99.42	2.13
2	1×10^{-14}	0.968×10^{-14}	96.83	3.63
3	1×10^{-13}	1.01×10^{-13}	100.5	6.56
4	1×10^{-12}	0.940×10^{-12}	93.98	3.05

4. CONCLUSION

In summary, by coupling the molecular biological technology and nanomaterials with electrochemical detection, this work achieved signal amplification based on target recycling and cascade catalysis to detect target miRNA-155. The CHA target recycling could be realized through a branch migration process without the assistance of nuclease. After target recycling, a large number of newly emerging fragments were produced, which were complementary to the S1-conjugated biobarcode NPs. S1-conjugated biobarcode NPs consisted of porous TiO_2 with high loading of PtNPs, S1, and Cyt *c*, exhibiting excellent biocompatibility and good electrocatalytic activity. Besides, S1 hybridized with AOx@Pt-labeled S2 to achieve cascade catalysis. The electrochemical response could be easily read out by intercalated redox mediator MB. With the above signal amplification strategies, the biosensor showed wide linear range and satisfying sensitivity for miRNA-155 detection, providing a promising way for the determination of miRNA in clinical applications.

■ ASSOCIATED CONTENT

Ⓢ Supporting Information

Signal amplification properties of CHA, mechanism of CHA, and optimization of detection condition. This material is available free of charge via the Internet at http://pubs.acs.org.

■ AUTHOR INFORMATION

Corresponding Authors
*Phone: +86-23-68252277. Fax: +86-23-68253172. E-mail: yuanruo@swu.edu.cn. (R.Y.)
*E-mail: yqchai@swu.edu.cn. (Y.-Q.C.)

Notes
The authors declare no competing financial interest.

■ ACKNOWLEDGMENTS

■ REFERENCES

(1) Dong, H. F.; Lei, J. P.; Ding, L.; Wen, Y. Q.; Ju, H. X.; Zhang, X. J. MicroRNA: Function, Detection, and Bioanalysis. *Chem. Rev.* **2013**, *113*, 6207−6233.

(2) Elton, T. S.; Selemon, H.; Elton, S. M.; Parinandi, N. L. Regulation of the MiR155 Host Gene in Physiological and Pathological Processes. *Gene* **2013**, *532*, 1−12.

(3) Medina, P. P.; Slack, F. J. MicroRNAs and Cancer. *Cell Cycle* **2008**, *7*, 2485−2492.

(4) Donnem, T.; Eklo, K.; Berg, T.; Sorbye, S. W.; Lonvik, K.; Saad, S. A.; Shibli, K. A.; Andersen, S.; Stenvold, H.; Bremnes, R. M.; Busund, L. T. Prognostic Impact of MiR-155 in Non-Small Cell Lung Cancer Evaluated by in Situ Hybridization. *J. Transl. Med.* **2011**, *9*, 6−14.

(5) Nelson, P. T.; Baldwin, D. A.; Scearce, L. M.; Oberholtzer, J. C.; Tobias, J. W.; Mourelatos, Z. Microarray-Based, High-Throughput Gene Expression Profiling of MicroRNAs. *Nat. Methods* **2004**, *1*, 155−161.

(6) Tanaka, K.; Tainaka, K.; Umemoto, T.; Nomura, A.; Okamoto, A. An Osmium-DNA Interstrand Complex: Application to Facile DNA Methylation Analysis. *J. Am. Chem. Soc.* **2007**, *129*, 14511−14517.

(7) Deng, H. M.; Shen, W.; Ren, Y. Q.; Gao, Z. Q. A Highly Sensitive MicroRNA Biosensor Based on Hybridized MicroRNA-Guided Deposition of Polyaniline. *Biosens. Bioelectron.* **2014**, *60*, 195−200.

(8) Zhou, Y. L.; Wang, M.; Xu, Z. N.; Ni, C. L.; Yin, H. S.; Ai, S. Y. Investigation of the Effect of Phytohormone on the Expression of MicroRNA-159a in Arabidopsis Thaliana Seedlings Based on Mimic Enzyme Catalysis Systematic Electrochemical Biosensor. *Biosens. Bioelectron.* **2014**, *54*, 244−250.

(9) Wu, X. Y.; Chai, Y. Q.; Yuan, R.; Su, H. L.; Han, J. A Novel Label-Free Electrochemical MicroRNA Biosensor Using Pd Nanoparticles as Enhancer and Linker. *Analyst* **2013**, *138*, 1060−1066.

(10) Shen, W.; Deng, H. M.; Ren, Y. Q.; Gao, Z. Q. A Real-Time Colorimetric Assay for Label-Free Detection of MicroRNAs Down to Sub-Femtomolar Levels. *Chem. Commun.* **2013**, *49*, 4959−4961.

(11) Radhakrishnan, S.; Sumathi, C.; Umar, A.; Kim, S. J.; Wilson, J.; Dharuman, V. Polypyrrole-Poly(3,4-ethylenedioxythiophene)-Ag(PPy-PEDOT-Ag) Nanocomposite Films for Label-Free Electrochemical DNA Sensing. *Biosens. Bioelectron.* **2013**, *47*, 133−140.

(12) Tran, H. V.; Piro, B.; Reisberg, S.; Tran, L. D.; Duc, H. T.; Pham, M. C. Label-Free and Reagentless Electrochemical Detection of MicroRNAs Using a Conducting Polymer Nanostructured by Carbon Nanotubes: Application to Prostate Cancer Biomarker MiR-141. *Biosens. Bioelectron.* **2013**, *49*, 164−169.

(13) Wang, L.; Hua, E. H.; Liang, M.; Ma, C. X.; Liu, Z. L.; Sheng, S. C.; Liu, M.; Xie, G. M.; Feng, W. L. Graphene Sheets, Polyaniline and AuNPs Based DNA Sensor for Electrochemical Determination of BCR/ABL Fusion Gene with Functional Hairpin Probe. *Biosens. Bioelectron.* **2014**, *51*, 201−207.

(14) Zhao, J.; Hu, S. S.; Zhong, W. D.; Wu, J. G.; Shen, Z. M.; Chen, Z.; Li, G. X. Highly Sensitive Electrochemical Aptasensor Based on a Ligase-Assisted Exonuclease III-Catalyzed Degradation Reaction. *ACS Appl. Mater. Interfaces* **2014**, *6*, 7070−7075.

(15) Yang, L.; Liu, C. H.; Ren, W.; Li, Z. P. Graphene Surface-Anchored Fluorescence Sensor for Sensitive Detection of MicroRNA Coupled with Enzyme-Free Signal Amplification of Hybridization Chain Reaction. *ACS Appl. Mater. Interfaces* **2012**, *4*, 6450−6453.

(16) He, Y. Q.; Zhang, N. N.; Gong, Q. J.; Li, Z. L.; Gao, J. P.; Qiu, H. X. Metal Nanoparticles Supported Graphene Oxide 3D Porous Monoliths and Their Excellent Catalytic Activity. *Mater. Chem. Phys.* **2012**, *134*, 585−589.

(17) Gu, Y.; Wu, H.; Xiong, Z. G.; Abdulla, W. A.; Zhao, X. S. The Electrocapacitive Properties of Hierarchical Porous Reduced Graphene Oxide Templated by Hydrophobic $CaCO_3$ Spheres. *J. Mater. Chem. A* **2014**, *2*, 451−459.

(18) Wen, D.; Guo, S. J.; Zhai, J. F.; Deng, L.; Ren, W.; Dong, S. J. Pt Nanoparticles Supported on TiO_2 Colloidal Spheres with Nanoporous Surface: Preparation and Use as an Enhancing Material for Biosensing Applications. *J. Phys. Chem. C* **2009**, *113*, 13023−13028.

(19) Suárez, G.; Santschi, C.; Martin, O. J. F.; Slaveykova, V. I. Biosensor Based on Chemically-Designed Anchorable Cytochrome *c* for the Detection of H_2O_2 Released by Aquaticcells. *Biosens. Bioelectron.* **2013**, *42*, 385−390.

(20) Bortolotti, C. A.; Paltrinieri, L.; Monari, S.; Ranieri, A.; Borsari, M.; Battistuzzi, G.; Sola, M. A Surface-Immobilized Cytochrome *c* Variant Provides a pH-Controlled Molecular Switch. *Chem. Sci.* **2012**, *3*, 807−810.

(21) Zhuo, Y.; Yuan, P. X.; Yuan, R.; Chai, Y. Q.; Hong, C. L. Bienzyme Functionalized Three-Layer Composite Magnetic Nano-

719

dx.doi.org/10.1021/am507059n | *ACS Appl. Mater. Interfaces* 2015, 7, 713−720

particles for Electrochemical Immunosensors. *Biomaterials* **2009**, *30*, 2284−2290.

(22) Han, J.; Zhuo, Y.; Chai, Y. Q.; Yu, Y. Q.; Liao, N.; Yuan, R. Electrochemical Immunoassay for Thyroxine Detection Using Cascade Catalysis as Signal Amplified Enhancer and Multi-Functionalized Magnetic Graphene Sphere as Signal Tag. *Anal. Chim. Acta* **2013**, *790*, 24−30.

(23) Azevedo, A. M.; Prazeres, D. M. F.; Cabral, J. M. S.; Fonseca, L. P. Ethanol Biosensors Based on Alcohol Oxidase. *Biosens. Bioelectron.* **2005**, *21*, 235−247.

(24) Wolfbeis, O. S.; Posch, H. E. Optical Sensors. *Anal. Bioanal. Chem.* **1988**, *332*, 255−257.

(25) Li, C. X.; Li, Y. X.; Xu, X.; Wang, X. Y.; Chen, Y.; Yang, X. D.; Liu, F.; Li, N. Fast and Quantitative Differentiation of Single-Base Mismatched DNA by Initial Reaction Rate of Catalytic Hairpin Assembly. *Biosens. Bioelectron.* **2014**, *60*, 57−63.

(26) Liu, S. F.; Wang, Y.; Ming, J. J.; Lin, Y.; Cheng, C. B.; Li, F. Enzyme-Free and Ultrasensitive Electrochemical Detection of Nucleic Acids by Target Catalyzed Hairpin Assembly Followed with Hybridization Chain Reaction. *Biosens. Bioelectron.* **2013**, *49*, 472−477.

(27) Chen, H. Y.; Ju, H. X.; Xun, Y. G. Methylene Blue/ Perfluorosulfonated Lonomer Modified Microcylinder Carbon Fiber Electrode and Its Application for the Determination of Hemoglobin. *Anal. Chem.* **1994**, *66*, 4538−4542.

(28) Kelley, S. O.; Barton, J. K. Electrochemistry of Methylene Blue Bound to a DNA-Modified Electrode. *Bioconjugate Chem.* **1997**, *8*, 31−37.

(29) Yan, M.; Sun, G. Q.; Liu, F.; Lu, J. J.; Yu, J. H.; Song, X. R. An Aptasensor for Sensitive Detection of Human Breast Cancer Cells by Using Porous GO/Au Composites and Porous PtFe Alloy as Effective Sensing Platform and Signal Amplification Labels. *Anal. Chim. Acta* **2013**, *798*, 33−39.

(30) Huang, M. H.; Shao, Y.; Sun, X. P.; Chen, H. J.; Liu, B. F.; Dong, S. J. Alternate Assemblies of Platinum Nanoparticles and Metalloporphyrins as Tunable Electrocatalysts for Dioxygen Reduction. *Langmuir* **2005**, *21*, 323−329.

(31) Jiang, X. C.; Herricks, T.; Xia, Y. N. Monodispersed Spherical Colloids of Titania: Synthesis, Characterization, and Crystallization. *Adv. Mater.* **2003**, *15*, 1205−1209.

(32) Wu, X. Y.; Chai, Y. Q.; Yuan, R.; Zhuo, Y.; Chen, Y. Dual Signal Amplification Strategy for Enzyme-Free Electrochemical Detection of MicroRNAs. *Sens. Actuators, B* **2014**, *203*, 296−302.

(33) Jiang, Y.; Li, B. L.; Milligan, J. N.; Bhadra, S.; Ellington, A. D. Real-Time Detection of Isothermal Amplification Reactions with Thermostable Catalytic Hairpin Assembly. *J. Am. Chem. Soc.* **2013**, *135*, 7430−7433.

(34) Zhang, D. Y.; Chen, S. X.; Yin, P. Optimizing the Specificity of Nucleic Acid Hybridization. *Nat. Chem.* **2012**, *4*, 208−214.

(35) Zheng, A. X.; Wang, J. R.; Li, J.; Song, X. R.; Chen, G. N.; Yang, H. H. Enzyme-Free Fluorescence Aptasensor for Amplification Detection of Human Thrombin via Target-Catalyzed Hairpin Assembly. *Biosens. Bioelectron.* **2012**, *36*, 217−221.

(36) Yuan, Y. L.; Chai, Y. Q.; Yuan, R.; Zhuo, Y.; Gan, X. X. An Ultrasensitive Electrochemical Aptasensor with Autonomous Assembly of Hemin-G-Quadruplex DNAzyme Nanowires for Pseudo Triple-Enzyme Cascade Electrocatalytic Amplification. *Chem. Commun.* **2013**, *49*, 7328−7330.

(37) Fang, S. P.; Lee, H. J.; Wark, A. W.; Corn, R. M. Attomole Microarray Detection of MicroRNAs by Nanoparticle-Amplified SPR Imaging Measurements of Surface Polyadenylation Reactions. *J. Am. Chem. Soc.* **2006**, *128*, 14044−14046.

(38) Cheng, Y.; Lei, J. P.; ChenY, L.; Ju, H. X. Highly Selective Detection of MicroRNA Based on Distance-Dependent Electro-chemiluminescence Resonance Energy Transfer Between CdTe Nanocrystals and Au Nanoclusters. *Biosens. Bioelectron.* **2014**, *51*, 431−436.

(39) Liu, H. Y.; Li, L.; Wang, Q.; Duan, L. L.; Tang, B. Graphene Fluorescence Switch-Based Cooperative Amplification: A Sensitive and Accurate Method to Detection MicroRNA. *Anal. Chem.* **2014**, *86*, 5487−5493.

(40) Liu, L.; Xia, N.; Liu, H. P.; Kang, X. J.; Liu, X. S.; Xue, C.; He, X. L. Highly Sensitive and Label-Free Electrochemical Detection of MicroRNAs Based on Triple Signal Amplification of Multifunctional Gold Nanoparticles, Enzymes and Redox-Cycling Reaction. *Biosens. Bioelectron.* **2014**, *50*, 399−405.

(41) Zhu, W. Y.; Su, X. P.; Gao, X. Y.; Dai, Z.; Zou, X. Y. A Label-Free and PCR-Free Electrochemical Assay for Multiplexed MicroRNA Profiles by Ligase Chain Reaction Coupling with Quantum Dots Barcodes. *Biosens. Bioelectron.* **2014**, *53*, 414−419.

(42) Peng, Y. L.; Jiang, J. H.; Yu, R. Q. A Sensitive Electrochemical Biosensor for MicroRNA Detection Based on Streptavidin-Gold Nanoparticles and Enzymatic Amplification. *Anal. Methods* **2014**, *6*, 2889−2893.